INVESTIGATION OF NOZZLES WITH CRYOGENIC BOUNDARY LAYER SUCTION

M. V. Prochukhaev

UDC 533.6.071.1

Results of an investigation of the characteristics of a carbon dioxide gas stream produced in supersonic nozzles with cryogenic boundary layer suction are presented.

At low gas stream densities the growth of a thick boundary layer on the nozzle walls produces great inconveniences in carrying out investigations. The absence of a sufficiently large isentropic nucleus results in complicating the experimental technique. Meanwhile, a lower limit of accessible Reynolds numbers, determined from the conditions of boundary layer closure, exists for each nozzle. It becomes difficult to reach hypersonic values of the Mach number in such nozzles [1]. One of the means to diminish the influence of near-wall viscous effects is cooling the nozzle wall to temperatures at which freezing of part of the working gas occurs [2].

Data available in the literature on the interaction between gas streams and cryogenic surfaces refer mainly to the case of flow around bodies [3, 5] and to the interaction of free jets with surfaces [4]. There are practically no results for internal flows.

We tried to investigate the characteristics of CO_2 condensation and the stream parameters in a supersonic nozzle with cryogenic boundary layer suction. To do this, we used three copper conical nozzles with identical critical section diameters ($d_* = 25$ mm), 49° and 10° half-angles of the subsonic and supersonic sections, respectively, and a $R = 50$ mm radius of curvature at the critical section. Starting with a distance of 15 mm from the critical section, the supersonic part in all the nozzles was cooled by liquid nitrogen. The diameters of the exit sections and the lengths of the supersonic portions were the following for the nozzles: nozzle No. 1 $D = 44$ mm, $L = 64$ mm; No. 2 $D = 50$ mm, $L = 81$ mm; No. 3 $D = 56$ mm, $L = 98$ mm, which corresponds to the geometric Mach numbers $M_{g1} = 2.5$; $M_{g2} = 2.77$; $M_{g3} = 3$. Nozzle No. 3 had four cooling sections whose gradual disconnection permitted investigation of the influence of the length of the cooled portion on the stream parameters.

In size, the perforated nozzle (nozzle No. 4) was identical to nozzle No. 3 however, the supersonic portion had perforations (1115 holes at a 2 mm diameter) starting with 18 mm from the critical section. The gas sucked out through the holes was frozen onto a cylindrical surface of 190 cm^2 area cooled by liquid nitrogen.

Carbon dioxide with a 0.2% volume fraction of impurities, supplied to the forechamber from a high-pressure tank through a heated reducer and an alumogel desiccant, was used as working gas. The carbon dioxide gas was heated to 480-500°K by using a tubular ohmic heater to prevent possible condensation during expansion in the nozzle. Liquid nitrogen was supplied from Dewar vessels under pressure to the nozzle cooling jacket. The liquid nitrogen discharge was 15 liters per hour. After evaporation in the cooling jacket, the gaseous nitrogen was vented to the atmosphere. The nozzle wall temperature during the experiments was 78°K.

The gas being accelerated in the nozzle was evacuated through a vacuum seal by a system of BN-4500 and BN-6G pumps.

Nozzles Nos. 1, 2, 3 had drainage holes along the generator of the supersonic part in order to measure the pressure, the pressure in nozzle No. 4 was measured at two points in the suction cavity: at a 18

Translated from Inzhenerno-Fizicheskii Zhurnal, Vol. 25, No. 1, pp. 87-93, July, 1973. Original article submitted December 8, 1972.

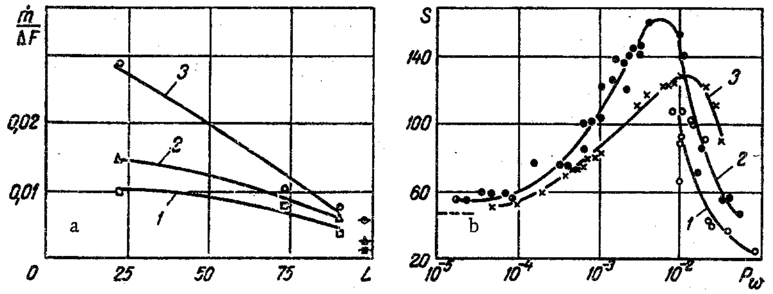

Fig. 1. Distribution of the mass condensation rate $\dot{m}/\Delta F$ kg /sec·m^2 over the nozzle length L, mm (a) and dependence of the volume condensation rate S, m/sec on the pressure at the wall P_W, mm Hg (b). The dashed line is the free molecular value of the condensation rate $S = 36.4\sqrt{T/\mu}$, m/sec.

mm distance from the critical section and at the nozzle exit. The pressure at the drainage points was measured first by a LT-2 converter calibrated by a MacLeod manometer to ±15% accuracy. The pressure in the forechamber ahead of the nozzle (P_0) was measured during the experiments by a U-shaped oil manometer as well as a manometer converter MT-6 to ±10-15% error. The pressure in the endface Pitot tube, to determine the stream Mach number, was measured by the same converter. The profile of the carbon dioxide frozen on the nozzle wall was also found. A thermocouple probe, which is a thermocouple fastened in a holder and mounted on a coordinate grid was used for this purpose.

The quantity of frozen carbon dioxide was determined as follows. After a specific drainage time, the gas supply ceased, the seal connecting the working chamber to the vacuum pumps was covered over and the electrical heating of the nozzle was switched on. The frozen carbon dioxide was evaporated and the pressure in the closed volume of the working chamber increased. The quantity of frozen gas was computed from the formula

$$m = (P_2/T_2 - P_1/T_1)\frac{V}{R}, \tag{1}$$

where P and T are the gas pressure and temperature in the working chamber, V is its volume, and R is the gas constant; the subscripts 1 and 2 refer to the state before and after the evaporation of CO_2. The total relative error in the determination of m was ±12%.

Determination of the Condensation Rate. A certain drop in the condensation rate with time was noted during the experiments, especially noticeable as the pressure increased, which is visibly associated with an increase in condensate thickness.

The use of three nozzles of different lengths (Nos. 1, 2, 3) permitted the determination of the mean mass rate of condensation over the area $\dot{m}/\Delta F = (\Delta m/\Delta\tau)/\Delta F$, in addition to the total quantity of frozen gas, where Δm is the quantity of gas frozen in the time $\Delta\tau$, ΔF is the difference between the areas of the nozzles investigated.

Experiments showed that the quantity $\dot{m}/\Delta F$ grows substantially as the critical section is approached for the whole pressure range studied (curve 1 in Fig. 1a has been obtained at the pressure $P_0 = 0.4$ mm Hg, 2) at $P_0 = 0.9$ mm Hg, 3) at $P_0 = 1.85$ mm Hg). Since the quantity $\dot{m}/\Delta F$ is proportional to the thickness of the frozen layer, the latter should also increase as the critical section is approached.

Only the mean value of $\dot{m}/\Delta F$ over the length could be determined for the perforated nozzle. The results of its determination, presented in the right side of Fig. 1a, indicate the lesser efficiency of the nozzle diagram with perforations. Reduction of the mass condensation rate occurs because of equilibration of the pressure in the freezing cavity and its diminution in the area of the critical section.

Measurement of the pressure distribution along the nozzle generator afforded the possibility of determining the magnitude of the volume condensation rate $S = (\Delta V/\Delta\tau)/\Delta F$, where ΔV is the volume of gas being frozen in the time $\Delta\tau$ at the pressure P_W; ΔF is the area. Since the nozzle wall temperature (T_W = 78°K) differs strongly from the temperature at which the pressure meter is operating (T = 293°K) during the pressure measurements, a thermotranspiration effect could be observed in the measuring channel. A calibration of the drainage channel showed, however, that the influence of this effect could be neglected for pressures $P_W < 2\cdot10^{-2}$ mm Hg for a 2 mm drainage hole diameter, a 10 mm measuring channel diameter, and a 100 mm length.

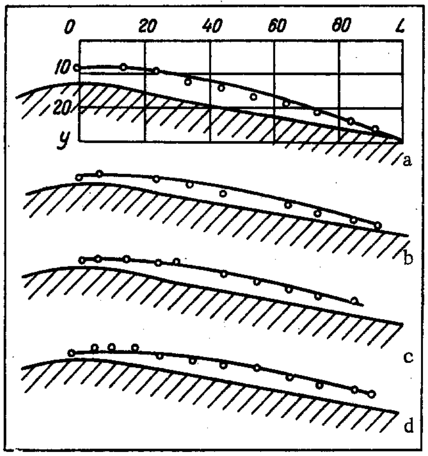

Fig. 2. Frozen gas profile y = f(L), mm.

Measurements of the volume condensation rate (curve 1 in Fig. 1b) showed that it depends essentially on the pressure. It should be noted that the achievable condensation rates for $P_W < 2 \cdot 10^{-2}$ mm Hg exceed the free-molecular value ($S = 36.4\sqrt{[T/\mu]}$, m/sec), which is visibly associated with the possibility of accelerating the gas in the direction to the walls. The drop in S as the pressure rises can be explained by an increase in the density in the gas layer near the wall, which should hinder the acceleration. The results of the present experiments agree satisfactorily with the results in [3] (curve 2 in Fig. 1b) obtained during condensation of CO_2 on the surface of a sphere, as well as with the results in [5] (curve 3) obtained during condensation of carbon dioxide on the surface of a disk.

Measurements of the frozen gas profile by using the thermocouple probe verified the deduction about the nonuniformity in growth of the condensate. The increase in condensate thickness as the critical section is approached (Fig. 2) because of the increase in the mass condensation rate results in a change in the actual nozzle geometry, and consequently, in a change in the stream parameters. To clarify the possibilities of diminishing this influence, condensate profiles were determined for different lengths (measuring from the exit) of the cooled portion of nozzle No. 3. The profiles measured after 20 min of operation are shown in Fig. 2 for a $P_0 = 0.9$ mm Hg stagnation pressure (a refers to the length L = 83 mm of the cooled portion, b to L = 63 mm, c to L = 42 mm, d to L = 21 mm). The profiles at the other pressures investigated were analogous. The observed diminution in the layer thickness at the critical section as the length of the cooled portion diminished is related to the rise in wall temperature and the consequent diminution in the condensation rate. An increase in the condensate thickness in the area of the nozzle exit is caused by a rise in static pressure.

Measurements of the condensation rate and condensate thickness permitted an estimation of its density. The mean value of the density of the carbon dioxide frozen at the temperature $T_W = 78°K$ was ≈ 2 g/cm^3.

Investigation of the Stream Characteristics. The specifics of operation of a nozzle with freezing which consists of a drop in the condensation rate with time on the one hand, and a change in the actual nozzle geometry with time on the other, should result in a change in the stream parameters at the nozzle exit. Here if the drop in the condensation rate should result in a diminution in the Mach number, then the change in geometry should result in a rise in the number M.

To establish the actual dependence, M was determined experimentally by using an endface Pitot tube with a d/D = 0.8 ratio between the hole and outer diameters. Since the probe readings depend on the degree of rarefaction, appropriate corrections were determined which agreed, in practice, with analogous corrections for air [6]. The influence noted above of the two factors (the change in condensation rate and the change in actual nozzle geometry) is seen clearly in Fig. 3a, where the change in the number M with time is shown for the three nozzle diagrams at $P_0 = 0.9$ mm Hg (curve 1 refers to nozzle No. 3 with a completely cooled supersonic part, 2 to nozzle No. 3 with cooling 42 mm from the exit, and 3 to the perforated nozzle). The initial abrupt rise in the number M for nozzle No. 3 is due to the appearance of powerful

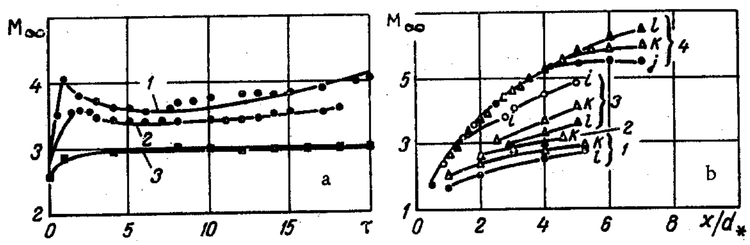

Fig. 3. Dependence of the Mach number on the time τ, min (a) and on the distance to the critical section x/d_* (b) for $P_0 = 0.3$ mm Hg (i), $P_0 = 0.5$ mm Hg (j), $P_0 = 0.9$ mm Hg (k), $P_0 = 1.85$ mm Hg (l).

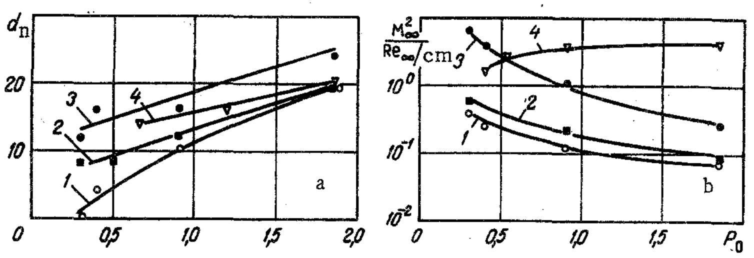

Fig. 4. Dependence of the stream nucleus diameter d_n, mm (a) and degree of rarefaction $M^2_\infty/Re_\infty/cm$ (b) on the stagnation pressure P_0, mm Hg.

cryogenic suction. Some further diminution in the number M is associated with the diminution in the condensation rate. However, after several minutes the growth in the condensate results in an increase in the ratio between the areas and a rise in the number M. As the length of the cooled part diminishes, fluctuations in the number M decrease, however, the numbers M reached also diminish because of the decrease in the fraction of frozen gas. The greatest stability in the number M is observed at the exit of the perforated nozzle, but for a lower general level of M it is true.

The transverse total pressure profiles vary toward a diminution in the diameter of the stream nucleus at the exit of a nozzle with freezing as time elapses. Because of the intense heat elimination to the wall, the question about the isentropy of the stream obtained arises in investigating a nozzle with freezing. Investigations of transverse temperature profiles by using a thermocouple probe showed that the existing temperature nucleus agrees approximately with the dynamic. The presence of temperature and dynamic nuclei canbe explained, despite the high values of the Knudsen number, by the slight influence of the reflected molecules on the stream characteristics because of the freezing of a significant portion on the nozzle walls and, therefore, it indicates no influence of viscosity and heat conduction on the stream parameters in the central part of the jet.

As follows from the results obtained, greater Mach numbers than the geometric are reached at some flow modes at the nozzle exit. To explain this fact, it can be assumed that the nozzle starts to operate as a discharge-geometric nozzle as the walls are cooled to the temperature at which freezing of the working gas occurs.

The relationship connecting the change in stream velocity to the external effects appears as follows in general form [7]:

$$(M^2-1)\frac{du}{u}=\frac{dA}{A}-\frac{dm}{m}-\frac{dL}{a^2}-\frac{\varkappa-1}{a^2}dQ-\frac{\varkappa}{a^2}dL_{fr}. \qquad (2)$$

In this case, the gas performs no work, hence dL = 0. Since the friction forces are substantial only in the domain near the wall, and exert no influence on stream acceleration at the axis in the presence of an isentropic nucleus, it can be assumed that $dL_{fr} = 0$. Intensive heat exchange is also limited by the boundary layer domain, hence dQ = 0. In this case, under the assumption of the isentropic nature of the flow, integration of (2) easily yields

$$\frac{\bar{A}}{\bar{m}}=\frac{\left(1+\frac{\varkappa-1}{2}M^2\right)^{\varkappa+1/2(\varkappa-1)}}{\left(\frac{\varkappa+1}{2}\right)^{\varkappa+1/2(\varkappa-1)}M}, \qquad (3)$$

where $\bar{A} = A/A_*$, $\bar{m} = m/m_*$, $m_* = m + m_b$, A is the nozzle area in the section under consideration, m is the gas discharge through this section, m_b is the discharge of the gas frozen on a portion prior to the section under consideration, and the subscript * refers to the critical section.

Computations carried out using (3) for nozzle No. 3 differ by 15% from the experimental values of the M numbers and, therefore, verify the assumption proposed above that a nozzle with cryogenic suction operates in the discharge-geometric mode.

To clarify the nature of the gas expansion in a nozzle with freezing, the stream characteristics produced by using the schemes described above are compared with the stream characteristics in a free CO_2 jet escaping from a sonic nozzle with sharp edges with a $d_* = 25$ mm hole diameter. Shown in Fig. 3b is the M number distribution along the stream axis for four acceleration schemes (conical nozzle without freezing – curve 1, perforated nozzle – 2, nozzle with freezing – 3, free jet – 4). An ordinary nozzle (grad M = 0-0.14 cm^{-1}) has the least gradient, and the free jet (grad M = 0.18-0.6 cm^{-1}) the greatest. The magnitude of grad M for a nozzle with freezing is 0.16 cm^{-1}. Spoilage of the self-similar dependence $M(x/d_*)$ for a free jet, starting with 2-3 calibers, occurs because of spoilage of the isentropy due to the influece of the longitudinal viscosity (see [8], for example). For these geometric dimensions this occurs for grad M = 0.18-0.5 cm^{-1} as a function of P_0. The fact that grad M is only 0.16 cm^{-1} at the exit of a nozzle with freezing at the minimal stagnation pressure asserts that the longitudinal viscosity does not shape the stream in this case.

The presence of intensive cryogenic suction results, as has been remarked above, in an increase in the stream nuclei. The nuclei obtained in a measurement by a Pitot tube are compared in Fig. 4a (notation is the same as in Fig. 3b). The domain in which the quantity P_0' varied by not more than 2% was taken as the magnitude of the nucleus. The stream nucleus for a free jet was determined provisionally at the section when spoilage of the isentropy occurred. A 12 mm diameter stream nucleus was fixed at the exit of a nozzle with freezing (curve 3) at a P_0 = 0.3 mm Hg pressure when joining of the boundary layers was observed in an ordinary nozzle.

One of the main demands imposed on a vacuum wind tunnel is the demand to obtain a stream with a high degree of rarefaction. In this case it is interesting to compare the greatest degree of rarefaction achieved in the nozzles investigated. Such a comparison is presented in Fig. 4 as the dependence $M^2_\infty/Re_{\infty 1cm} = f(P_0)$. A computation of M^2_∞/Re_∞ for a free jet was performed at that distance from the exit where the assumption about isentropy was still valid. The comparison indicates the possibility of more than one order of magnitude increase in M^2_∞/Re_∞ because of using boundary layer freezing. Use of a free jet can also yield a substantial gain in investigations admitting of high longitudinal gradients.

NOTATION

ρ, u, P, T are the density, velocity, pressure, and temperature;
M is the Mach number;
Re is the Reynolds number;
V is the working chamber volume;
μ is the molecular weight of the gas;
m is the mass of gas;
τ is the time;
F is the area of the nozzle side surface;
A is the nozzle cross-section;
L is the nozzle length;
D is the diameter;
S is the volume rate of condensation.

Superscripts

∞ denotes the free stream parameters;
0 denotes the adiabatically frozen gas parameters;
' denotes the parameters behind the normal compression shock;
* denotes the parameters in the nozzle critical section.

LITERATURE CITED

1. V. P. Agafonov, Izv. Akad. Nauk SSSR, Mekhanika, No. 5 (1965).
2. W. N. MacDermott, B. H. Shirley, and R. E. Dix, Rarefied Gas Dynamics, 2 (1966).
3. E. Mayer and R. Tracy, Rarefied Gas Dynamics, 2 (1966).
4. E. G. Velikanov and A. K. Rebrov, Izv. SO AN SSSR, Ser. Tekh. Nauk, 3, No. 13 (1970).
5. E. G. Velikanov and A. K. Rebrov, Inzh. Fiz. Zh., 20, No. 2 (1971).
6. V. A. Sukhnev, Izv. Akad. Nauk SSSR, Mekhan. i Mashinostroenie, No. 5 (1964).
7. G. N. Abramovich, Applied Gas Dynamics [in Russian], Nauka, Moscow (1969).
8. M. N. Kogan, Rarefied Gas Dynamics [in Russian], Nauka, Moscow (1967).